Biochimica et Biophysica Acta 1798 (2010) 1153–1163

Contents lists available at ScienceDirect

Biochimica et Biophysica Acta

journal homepage: www.elsevier.com/locate/bbamem

Interaction of 18-methoxycoronaridine with nicotinic acetylcholine receptors in different conformational states

Hugo R. Arias [a,*], Avraham Rosenberg [b], Dominik Feuerbach [c], Katarzyna M. Targowska-Duda [d], Ryszard Maciejewski [e], Krzysztof Jozwiak [d], Ruin Moaddel [b], Stanley D. Glick [f], Irving W. Wainer [b]

[a] Department of Pharmaceutical Sciences, College of Pharmacy, Midwestern University, Glendale, Arizona, USA
[b] Gerontology Research Center, National Institute of Aging, NIH, Baltimore, USA
[c] Neuroscience Research, Novartis Institutes for Biomedical Research, Basel, Switzerland
[d] Department of Chemistry, Medical University of Lublin, Lublin, Poland
[e] linical Neuroengineering Center, Medical University of Lublin, Lublin, Poland
[f] Center for Neuropharmacology and Neuroscience, The Albany Medical College, Albany, NY, USA

ARTICLE INFO

Article history:
Received 5 November 2009
Received in revised form 10 March 2010
Accepted 12 March 2010
Available online 19 March 2010

Keywords:
Nicotinic acetylcholine receptor
Conformational state
Noncompetitive antagonist
Ibogaine analog
18-Methoxycoronaridine

ABSTRACT

The interaction of 18-methoxycoronaridine (18-MC) with nicotinic acetylcholine receptors (AChRs) was compared with that for ibogaine and phencyclidine (PCP). The results established that 18-MC: (a) is more potent than ibogaine and PCP inhibiting (±)-epibatidine-induced AChR Ca^{2+} influx. The potency of 18-MC is increased after longer pre-incubation periods, which is in agreement with the enhancement of [^{3}H]cytisine binding to resting but activatable *Torpedo* AChRs, (b) binds to a single site in the *Torpedo* AChR with high affinity and inhibits [^{3}H]TCP binding to desensitized AChRs in a steric fashion, suggesting the existence of overlapping sites. This is supported by our docking results indicating that 18-MC interacts with a domain located between the serine (position 6′) and valine (position 13′) rings, and (c) inhibits [^{3}H]TCP, [^{3}H] ibogaine, and [^{3}H]18-MC binding to desensitized AChRs with higher affinity compared to resting AChRs. This can be partially attributed to a slower dissociation rate from the desensitized AChR compared to that from the resting AChR. The enthalpic contribution is more important than the entropic contribution when 18-MC binds to the desensitized AChR compared to that for the resting AChR, and vice versa. Ibogaine analogs inhibit the AChR by interacting with a luminal domain that is shared with PCP, and by inducing desensitization.

1. Introduction

Nicotinic acetylcholine receptors (AChRs) are members of the Cys-loop ligand-gated ion channel superfamily that also includes types A and C γ-aminobutyric acid (GABA), type 3 5-hydroxytryptamine (serotonin), and glycine receptors (reviewed in [1–5]). The alkaloid ibogaine and its natural and synthetic analogs behave pharmacologically as noncompetitive antagonists (NCAs) of several AChRs [6–8]. It has been hypothesized that this inhibitory activity is related to their anti-addictive properties [8–12]. In particular, 18-methoxycoronaridine (18-MC) has higher specificity for the α3β4 AChR [9]. This receptor subtype is expressed in relatively high amounts in the habenulo-interpeduncular pathway which modulates the mesocorticolimbic pathway, the so-called "brain reward circuitry" [8–11]. Considering this evidence, possible roles for AChRs in the process of drug addiction and consequently as targets for the pharmacological action of anti-addictive drugs have been suggested [10].

A better understanding of the interaction of ibogaine analogs with AChRs is crucial to develop novel compounds for safer anti-addictive therapies. However, we do not have structural and functional information on the interaction of 18-MC with its binding site(s) when the AChR is in different conformational states, especially considering that AChR desensitization seems to play an important role in the process of drug addiction (reviewed in [13]). As a first attempt to study this interaction we chose the muscle-type AChR because it is the archetype of the Cys-loop ligand-gated ion channel superfamily and because we can manipulate the different receptor conformational states in a variety of *in vitro* assays. We also used this particular AChR type because the binding site locations of several NCAs have already been characterized, including that for phencyclidine (PCP) [14–19] (reviewed in [3]). Taking advantage of this previous knowledge, the mutual interaction between 18-MC and PCP in the AChR is compared. To refine our understanding of the interaction between 18-MC and the AChR, we compared this interaction with that for ibogaine, the archetype of this family of

* Corresponding author. Department of Pharmaceutical Sciences, College of Pharmacy, Midwestern University, 19555 N. 59th Ave., Glendale, AZ 85308, USA. Tel.: +1 623 572 3589; fax: +1 623 572 3550.
E-mail address: harias@midwestern.edu (H.R. Arias).

0005-2736/$ – see front matter © 2010 Elsevier B.V. All rights reserved.
doi:10.1016/j.bbamem.2010.03.013

drugs. To accomplish these objectives, we used biochemical and functional approaches including radioligand binding assays employing several NCAs {i.e., [^{3}H]18-MC, [^{3}H]ibogaine, and [^{3}H]TCP, the analog of PCP, [piperidyl-3, 4-^{3}H(*N*)]-*N*-(1-(2 thienyl)cyclohexyl)-3,4-piperidine} and the agonist [^{3}H]cytisine, as well as Ca^{2+} influx assays, kinetics and thermodynamic measurements, and molecular modeling and docking studies. Although this study does not intend to determine the anti-addictive properties of ibogaine analogs, the results from this work will pave the way for a better understanding of how these compounds interact with the AChR.

2. Materials and methods

2.1. Materials

[Piperidyl-3, 4-^{3}H(*N*)]-(*N*-(1-(2 thienyl)cyclohexyl)-3,4-piperidine) ([^{3}H]TCP; 45 Ci/mmol), and [^{3}H]cytisine hydrochloride (35.6 Ci/mmol) were obtained from PerkinElmer Life Sciences Products, Inc. (Boston, MA, USA), and stored in ethanol at −20 °C. [^{3}H]18-Methoxycoronaridine ([^{3}H]18-MC; 25 Ci/mmol) was prepared by American Radiolabeled Chemicals Inc. (Saint Louis, MO, USA) by tritium labeling of the 18-methoxycoronaridine hydrochloride salt synthesized as previously described [12]. [^{3}H]Ibogaine (23 Ci/mmol), ibogaine hydrochloride, and phencyclidine hydrochloride (PCP) were obtained through the National Institute on Drug Abuse (NIDA) (NIH, Baltimore, USA). Carbamylcholine chloride (CCh), suberyldicholine dichloride, pepstatin A, leupeptin, aprotinin, calpain I, calpain II, benzamidine, cholesterol, phosphatidylserine, sphingomyelin, phosphatidic acid, phenylmethylsulfonyl fluoride (PMSF), polyethylenimine, sodium cholate, bovine serum albumin (BSA), and (±)-epibatidine were purchased from Sigma Chemical Co. (St. Louis, MO, USA). α-Bungarotoxin (α-BTx) was obtained from Invitrogen Co. (Carlsbad, CA, USA). [1-(Dimethylamino) naphtalene-5-sulfonamido] ethyltrimethylammonium perchlorate (dansyltrimethylamine) was purchased from Pierce Chemical Co. (Rockford, IL, USA). Fetal bovine serum and trypsin/EDTA were purchased from Gibco BRL (Paisley, UK). Salts were of analytical grade.

2.2. Preparation of Torpedo AChR native membranes, cellular membrane affinity chromatography (CMAC) column, and chromatographic system

AChR native membranes were prepared from frozen *Torpedo californica* electric organs obtained from Aquatic Research Consultants (San Pedro, CA, USA) by differential and sucrose density gradient centrifugation, as described previously [20]. Total AChR membrane protein was determined by using the bicinchoninic acid protein assay (Thermo Fisher Scientific, Rockford, IL, USA). Specific activities of these membrane preparations were determined by the decrease in dansyltrimethylamine (6.6 μM) fluorescence produced by the titration of suberyldicholine into receptor suspensions (0.3 mg/mL) in the presence of 100 μM PCP and ranged from 1.0 to 1.2 nmol of suberyldicholine binding sites/mg total protein (0.5–0.6 nmol AChR/mg protein). The AChR membrane preparations were stored at −80 °C in 20% sucrose.

The CMAC-*Torpedo* AChR column was prepared by immobilization of solubilized *Torpedo* AChR membranes following a previously described protocol [21,22]. *Torpedo* AChR membranes (500 mg) were first homogenized in buffer A (50 mM Tris–HCl buffer, pH 7.4, containing 1 mM pepstatin A, 20 μM leupeptin, 1 mM aprotinin, 1 mM calpain I, 1 mM calpain II, 1 mM benzamidine, 2 mM $MgCl_2$, 3 mM $CaCl_2$, 100 mM NaCl, 5 mM KCl, and 0.2 mM PMSF), and subsequently solubilized in buffer A containing 2% (w/v) sodium cholate and 10% (v/v) glycerol, in the presence of 100 nM cholesterol, 60 μM phosphatidylserine, 20 μM sphingomyelin, and 60 μM phosphatidic acid. Then, 200 mg of the Immobilized Artificial Monolayer (IAM) liquid chromatographic stationary phase (ID = 12 μM, 300 Å pore; Regis Chemical Co.) was suspended in the supernatant, and the mixture was rotated at room temperature (RT) for 1 h. The suspension was dialyzed for 1 day against 1 L of 50 mM Tris–saline buffer, pH 7.4, containing 5 mM EDTA, 100 mM NaCl, 0.1 mM $CaCl_2$, and 0.1 mM PMSF. The suspension was then centrifuged at 700 ×*g* at 4 °C and the pellet (*Torpedo*-IAM) was washed three times with 10 mM ammonium acetate buffer, pH 7.4. The stationary phase was packed into a HR 5/2 column (GE Healthcare, Piscataway, NJ, USA) to yield a 150 mM × 5 mM (ID) chromatographic bed, the CMAC-*Torpedo* AChR column.

Finally, the CMAC-*Torpedo* AChR column was attached to the chromatographic system Series 1100 Liquid Chromatography/Mass Selective Detector (Agilent Technologies, Palo Alto, CA, USA) equipped with a vacuum de-gasser (G 1322 A), a binary pump (1312 A), an autosampler (G1313 A) with a 20 μL injection loop, a mass selective detector (G1946 B) supplied with atmospheric pressure ionization electrospray and an on-line nitrogen generation system (Whatman, Haverhill, MA, USA). The chromatographic system was interfaced to a 250 MHz Kayak XA computer (Hewlett-Packard, Palo Alto, CA, USA) running ChemStation software (Rev B.10.00, Hewlett-Packard).

A 10 μL sample of 10 μM 18-MC was injected onto the CMAC-*Torpedo* AChR column, and the alkaloid was monitored in the positive ion mode using single ion monitoring at $m/z = 369.1$ $[MW+H]^+$ ion with the capillary voltage at 3000 V, the nebulizer pressure at 35 psi, and the drying gas flow at 11 L/min at a temperature of 350 °C.

2.3. Ca^{2+} influx measurements in TE671 cells expressing human fetal muscle AChRs

The TE671 cell line is a human rhabdomyosarcoma cell line (obtained from American Type Culture Collection, USA) that endogenously expresses the human fetal muscle AChR (i.e., α1β1γδ). This receptor subtype has the same subunit composition as the *Torpedo* AChR and thus, comparative correlations can be assessed. TE671 cells were cultured in a 1:1 mixture of Dulbecco's Modified Eagle Medium (DMEM) and Ham's F-12 Nutrient Mixture (Seromed, Biochrom, Berlin, Germany), supplemented with 10% (v/v) fetal bovine serum, as previously described [22–24]. DMEM/Ham's F-12 contains 1.2 g/L $NaHCO_3$, 3.2 g/L sucrose, and stable glutamine (L-Alanyl-L-Glutamine, 524 mg/L). The cells were incubated at 37 °C, 5% CO_2 and 95% relative humidity. The cells were passaged every 3 days, by detaching the cells from the culture flask by washing with phosphate-buffered saline and brief incubation (3–5 min) with trypsin (0.5 mg/mL)/EDTA (0.2 mg/mL).

Ca^{2+} influx was determined as previously described [22–24]. Briefly, 5×10^4 TE671 cells per well were seeded 72 h prior to the experiment on black 96-well plates (Costar, New York, USA) and incubated at 37 °C in a humidified atmosphere (5% CO_2/95% air). 16–24 h before the experiment, the medium was changed to 1% BSA in HEPES-buffered salt solution (HBSS) (130 mM NaCl, 5.4 mM KCl, 2 mM $CaCl_2$, 0.8 mM $MgSO_4$, 0.9 mM NaH_2PO_4, 25 mM glucose, 20 mM HEPES, pH 7.4). On the day of the experiment, the medium was removed by flicking the plates and replaced with 100 μL HBSS/1% BSA containing 2 μM Fluo-4 (Molecular Probes, Eugene, Oregon, USA) in the presence of 2.5 mM probenecid (Sigma, Buchs, Switzerland). The cells were then incubated at 37 °C in a humidified atmosphere (5% CO_2/95% air) for 1 h. Plates were flicked to remove excess of Fluo-4, washed twice with HBSS/1% BSA, and finally refilled with 100 μL of HBSS containing different concentrations of the ligand under study, and pre-incubated for 5 min, or for 4 and 24 h in the case of 18-MC. To determine the inhibitory mechanism for 18-MC, additional experiments were performed by pre-incubating the cells with 1, 10, and 100 μM 18-MC, respectively, before the (±)-epibatidine-induced Ca^{2+} influx determinations.

Plates were then placed in the cell plate stage of the fluorimetric imaging plate reader (FLIPR) (Molecular Devices, Sunnyvale, CA, USA). A baseline consisting of 5 measurements of 0.4 s each was recorded. (±)-Epibatidine (1 μM) was then added from the agonist plate to the cell plate using the FLIPR 96-tip pipettor simultaneously to fluorescence recordings for a total length of 3 min. The laser excitation and emission wavelengths are 488 and 510 nm, at 1 W, and a CCD camera opening of 0.4 s.

2.4. Equilibrium binding of [^{3}H]18-MC to the Torpedo AChR

In order to determine the binding affinity of [^{3}H]18-MC for the *Torpedo* AChR, equilibrium binding assays were performed as previously described [15]. Briefly, *Torpedo* AChR native membranes (0.5 μM) were suspended in binding saline (BS) buffer (50 mM Tris–HCl, 120 mM NaCl, 5 mM KCl, 2 mM $CaCl_2$, 1 mM $MgCl_2$, pH 7.4), in the presence of 1 mM CCh (desensitized/CCh-bound state), and pre-incubated for 30 min at RT. The [^{3}H]18-MC equilibrium binding to the resting AChR could not be determined because of a higher noise/signal level. The total volume of the membrane suspensions (total and nonspecific binding) was divided into aliquots and increasing concentrations of [^{3}H]18-MC + 18-MC (i.e., 0.07 nM–1.2 μM) were added to each tube and incubated for 2 h at RT. Nonspecific binding was determined in the presence of 100 μM 18-MC. Specific binding was calculated as total binding (no 18-MC) minus nonspecific binding (in the presence of 18-MC). AChR-bound [^{3}H]18-MC was then separated from free radioligand by a filtration assay using a 48-sample harvester system with GF/B Whatman filters (Brandel Inc., Gaithersburg, MD, USA), previously soaked with 0.5% polyethylenimine for 30 min. The membrane-containing filters were transferred to scintillation vials with 3 mL of Bio-Safe II (Research Product International Corp, Mount Prospect, IL, USA), and the radioactivity was determined using a Beckman 6500 scintillation counter (Beckman Coulter, Inc., Fullerton, CA, USA).

Using the Prism software (GraphPad Software, San Diego, CA, USA), binding data were fitted according to the Rosenthal–Scatchard equation [25]:

$$[B]/[F] = -([B]/K_d) + (B_{max}/K_d) \quad (1)$$

where the dissociation constant (K_d) for [^{3}H]18-MC is obtained from the negative reciprocal of the slope. The stoichiometry of [^{3}H]18-MC binding sites in the membrane preparation can be estimated from the *x*-intersect (when $y = 0$) of the plot $[B]/[F]$ *versus* $[B]$, where the obtained value corresponds to the number of [^{3}H]18-MC binding sites (B_{max}) per the used concentration of total proteins (0.5 μM).

2.5. Radioligand binding experiments using Torpedo AChRs in different conformational states

To determine the binding affinity of ibogaine analogs for the *Torpedo* AChR ion channel, the influence of 18-MC on [^{3}H]TCP binding, the effect of PCP, ibogaine, and 18-MC on [^{3}H]18-MC binding, and the effect of 18-MC on [^{3}H]ibogaine binding to *Torpedo* AChRs in different conformational states was studied. In this regard, AChR native membranes (0.3 μM) were suspended in BS buffer with 7 nM [^{3}H]TCP or 3.6 nM [^{3}H]18-MC or 19 nM [^{3}H]ibogaine in the presence of 1 mM CCh (desensitized/CCh-bound state), or with 15 nM [^{3}H]TCP or 5.5 nM [^{3}H]18-MC in the presence of 1 μM α-BTx (resting/α-BTx-bound state), and pre-incubated for 30 min at RT. α-Bungarotoxin is a competitive antagonist that maintains the AChR in the resting (closed) state [26]. Nonspecific binding was determined in the presence of 50 μM PCP (for the [^{3}H]TCP and [^{3}H]ibogaine experiments in the desensitized/CCh-bound state), 50 μM 18-MC (for the [^{3}H]18-MC experiments in the desensitized/CCh-bound state), or of 100 μM PCP or 100 μM 18-MC (for the [^{3}H]TCP and [^{3}H]18-MC experiments in the resting/α-BTx-bound state, respectively), as was used previously [14–17,22,24].

To determine whether 18-MC and ibogaine modulate agonist binding to AChRs, *Torpedo* AChR membranes (0.3 μM) were incubated with 7.7 nM [^{3}H]cytisine in the resting but activatable state (no other ligand present) as described previously [24]. The nonspecific binding was determined in the presence 1 mM CCh.

The total volume was divided into aliquots, and increasing concentrations of the ligand under study were added to each tube and incubated for 2 h at RT. AChR-bound radioligand was then separated from free radioligand by using the filtration assay described in Section 2.4.

The concentration–response data were curve-fitted by non-linear least-squares analysis using the Prism software. The corresponding IC_{50} values were calculated using the following equation:

$$\theta = 1/\left[1 + ([L]/IC_{50})^{n_H}\right] \quad (2)$$

where θ is the fractional amount of the radioligand bound in the presence of inhibitor at a concentration $[L]$ compared to the amount of the radioligand bound in the absence of inhibitor (total binding). IC_{50} is the inhibitor concentration at which $\theta = 0.5$ (50% bound), and n_H is the Hill coefficient. The n_H values were summarized in Table 2.

The observed IC_{50} values from the competition experiments described above were transformed into inhibition constant (K_i) values using the Cheng–Prusoff relationship [27]:

$$K_i = IC_{50}/\left\{1 + \left([ligand]/K_d^{ligand}\right)\right\} \quad (3)$$

where [ligand] is the initial concentration of the used radioligand (i.e., [^{3}H]TCP, [^{3}H]18-MC, [^{3}H]ibogaine), and K_d^{ligand} is the dissociation constant for [^{3}H]TCP in the resting (0.83 μM; [15]) and desensitized (0.25 μM; [28]) states, [^{3}H]ibogaine (5.4 μM; [29]), and [^{3}H]18-MC in the desensitized state (0.23 μM, see Fig. 2). The value for [^{3}H]18-MC in the resting state was taken from the [^{3}H]TCP competition experiments (1.4 μM, see Table 2). In addition, the free energy change (ΔG) for the interaction of the NCAs with the receptor was determined using the following equation (reviewed in [1]):

$$\Delta G = RT \ln K_i \quad (4)$$

where R is the gas constant (8.3145 J mol^{-1} K^{-1}), and T is the experimental temperature in Kelvin (293 K). The calculated K_i and ΔG values for the NCAs were summarized in Table 2.

2.6. Schild-type analysis for 18-MC-induced inhibition of [^{3}H]TCP binding

To have a better indication whether 18-MC inhibits [^{3}H]TCP binding to the desensitized AChR by a steric or allosteric mechanism, 18-MC-induced inhibition of [^{3}H]TCP binding experiments were performed at increasing initial concentrations of unlabeled PCP (i.e., 0, 3.1, 6.3, and 9.4 μM, respectively). The rationale of this experiment is based on the expectation that, for a higher initial concentration of the radioligand, a higher concentration of the competitor will be necessary to produce a total inhibition of radioligand binding. This is consistent with Schild-type analysis [30]. From these competition curves the apparent IC_{50} values were obtained from the plots according to Eq. (2). Then, we plot the ratio between the IC_{50} values for 18-MC determined at different initial concentrations of unlabeled PCP under the IC_{50} control values (no PCP added) *versus* the initial PCP concentration ($IC_{50}^{18\text{-MC}}/IC_{50}^{control}$ *versus* $[PCP]_{initial}$) (for more details see [14]). A linear relationship from this modified Schild-type plot would indicate a competitive interaction, whereas a non-linear relationship would suggest an allosteric mechanism of inhibition [14,30].

2.7. Determination of the binding kinetics for 18-MC using non-linear chromatography

To determine the kinetic parameters for 18-MC, chromatographic elutions of 18-MC from the CMAC-*Torpedo* AChR column were carried out using a mobile phase composed of 10 mM ammonium acetate buffer (pH 7.4):methanol (85:15, v/v) delivered at a flow rate of 0.2 mL/min at 20 °C, as described previously [21,22]. The first set of experiments was performed in the presence of 1 nM α-BTx (the AChR is mainly in the resting state; see [26]), and a second set of experiments was determined in parallel in the presence of 0.1 μM (±)-epibatidine (the AChR is mainly in the desensitized state).

In the non-linear chromatography approach, concentration-dependent asymmetric chromatographic traces are observed due to slow adsorption/desorption rates. The mathematical approach used in this study to resolve these non-linear conditions was the Impulse Input Solution [31]. The chromatographic data were analyzed using PeakFit v4.12 for Windows Software (SPSS Inc., Chicago, IL, USA) following a previously reported protocol [21,32]. The details of this approach and its application to the determination of the binding kinetics of NCAs to neuronal AChRs were presented earlier [21,32,33]. Briefly, the resultant peaks were fitted to the Impulse Input Solution model by adjusting four variables, namely a_0–a_3. The a_2 variable was directly used for the calculation of the dissociation rate constant (k_{off}) according to this equation:

$$k_{off} = 1/(a_2 t_0) \tag{5}$$

where the dead time of the column, t_0, is determined as the time required for the elution of water. The a_3 value was used to calculate the association constant (K_a) for the formation of the ligand-receptor complex in equilibrium using this relationship:

$$K_a = a_3/[18 - MC] \tag{6}$$

where [18-MC] is the concentration of 18-MC. Both K_a and k_{off} values can be used to further calculate the association rate constant, k_{on} ($k_{on} = K_a \cdot k_{off}$).

2.8. Thermodynamic parameters for the interaction of 18-MC with Torpedo AChRs

The chromatographic elution of 18-MC from the CMAC-*Torpedo* AChR column was carried out as explained in Section 2.7 at the following temperatures: 10, 12, 16, 20, and 25 °C. For the temperature-dependence studies, van't Hoff plots were constructed according to the following linear regression equation (reviewed in [1]):

$$\ln K_a = (\Delta S^\circ/R) - (\Delta H^\circ/R)(1/T), \tag{7}$$

where the K_a values were obtained using Eq. (6), and ΔS° and ΔH° are the standard entropy change and standard enthalpy change, respectively. These parameters were calculated using the slope ($\Delta H^\circ = -\text{Slope}\cdot R$) and y-intersect ($\Delta S^\circ = y\text{-intersect}\cdot R$) values from the plots. In addition, the entropic contribution was calculated as $-T\Delta S^\circ$, and the free energy change at 293K (ΔG^{20}) was calculated using the Gibbs–Helmholtz equation (reviewed in [1]):

$$\Delta G^{20} = \Delta H^\circ - T\Delta S^\circ. \tag{8}$$

The k_{off} values obtained using Eq. (5) were also used to construct the Arrhenius plots to determine the energy of activation (E_a) of the dissociation process, according to the Arrhenius equation (reviewed in [1]):

$$\ln k_{off} = \ln A - (E_a/R)(1/T), \tag{9}$$

where A is the Arrhenius or pre-exponential factor, and E_a was determined from the slope of the plot ($E_a = -\text{Slope}\cdot R$). In turn, the E_a values were used to calculate the enthalpy change of the transition state (ΔH^+) according to the following equation (reviewed in [1]):

$$\Delta H^+ = E_a - RT. \tag{10}$$

2.9. Molecular docking of 18-MC in muscle-type AChR ion channels

Amino acid sequences in the M2 transmembrane segments of the AChR ion channel are highly conserved between different species and subunits. However, the absolute numbering of amino acid residues varies greatly between subunits, thus, the residues in M2 of AChR subunits are referred to here using the prime nomenclature (1′ to 20′) corresponding to residues Met^{243} to Glu^{262} in the *Torpedo* AChR α1-subunit. As binding targets for modeling we first used a structural model of the pore region of AChR based on the cryo-electron microscopy structure of the *Torpedo* AChR determined at ~4 Å resolution (PDB ID 2BG9) [34,35]. Subsequently, a model of the human muscle AChR subtype was constructed applying homology/comparative modeling methods on the *Torpedo* 2BG9 as a template.

Computational simulations were performed using the same protocol as recently reported [17,22]. In the first step, 18-MC molecules in either the protonated or neutral form were sketched using HyperChem 6.0 (HyperCube Inc., Gainesville, FL), optimized using the semiempirical method AM1 (Polak–Ribiere algorithm to a gradient lower than 0.1 kcal/Å/mol), and then transferred for the subsequent step of ligand docking. The Molegro Virtual Docker (MVD 2008.2.4.0 Molegro ApS Aarhus, Denmark) was used for docking simulations of flexible ligands into the rigid target AChR model. The docking space was limited and centered in the middle of the ion channel and extended enough to ensure covering of the whole channel domain for sampling simulations (docking space was defined as a sphere of 21 Å in diameter). The actual docking simulations were performed using the following settings: numbers of runs = 100; maximal number of iterations = 10,000; maximal number of poses = 10, and the pose representing the lowest value of the scoring function (MolDockScore) for 18-MC was further analyzed.

3. Results

3.1. Inhibition of (±)-epibatidine-mediated Ca^{2+} influx in TE671 cells by 18-MC, ibogaine, and phencyclidine

Since there is no previous information about the interaction of ibogaine analogs with muscle AChRs, Ca^{2+} influx experiments were performed to compare the inhibitory potency of 18-MC with that for ibogaine and PCP. First, the activation potency of (±)-epibatidine was determined ($EC_{50} = 0.26 \pm 0.04$ μM; Fig. 1) by following the fluorescence increase in TE671-hα1β1γδ AChR cells produced by (±)-epibatidine-induced Ca^{2+} influx as described previously [22,24]. To compare the inhibitory potency (IC_{50}) of 18-MC, ibogaine and PCP, TE671 cells were pre-incubated (5 min) with each ligand and their inhibitory properties were assessed by (±)-epibatidine-induced Ca^{2+} influx experiments (Fig. 1A). The observed values for ibogaine (17.0 ± 3.0 μM) and PCP (31.0 ± 2.0 μM) (Table 1) were statistically identical to that obtained by $^{86}Rb^+$ efflux experiments using the same human muscle AChR [7]. Our results indicate that 18-MC (6.8 ± 0.8 μM) is ~2-fold more potent than ibogaine, the archetypical member of this family of drugs,

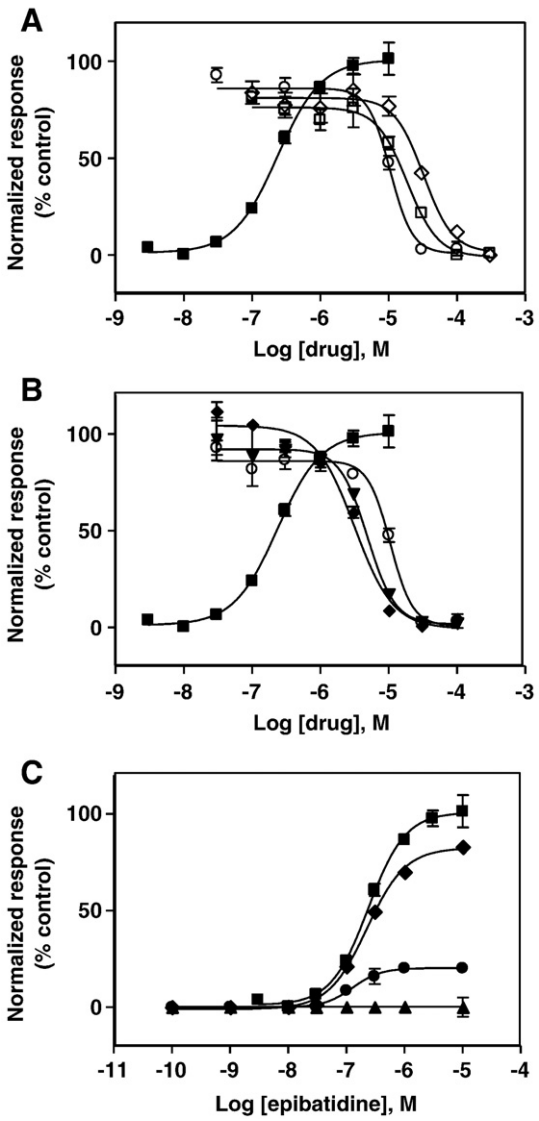

Fig. 1. Effect of 18-methoxycoronaridine (18-MC), ibogaine, and PCP on (±)-epibatidine-induced calcium influx in TE671-hα1β1γδ cells. (A) Increased concentrations of (±)-epibatidine (■) activate the hα1β1γδ AChR with potency $EC_{50} = 0.26 \pm 0.04$ μM ($n_H = 1.23 \pm 0.06$). Subsequently, cells were pre-treated for 5 min with several concentrations of 18-MC (○), ibogaine (□), and PCP (◊) followed by addition of 1 μM (±)-epibatidine. (B) Longer pre-treatment increases the inhibitory potency of 18-MC on (±)-epibatidine-induced calcium influx in TE671-hα1β1γδ cells. Pre-treatment periods were: 5 min (○), 4 h (▼), and 24 h (♦), respectively. Responses in both plots were normalized to the maximal (±)-epibatidine response which was set as 100%. The calculated IC_{50} and n_H values are summarized in Table 1. (C) Pre-treatment with 1 (♦), 10 (●), and 100 μM 18-MC (▲), respectively, inhibits (±)-epibatidine-induced calcium influx in TE671-hα1β1γδ cells in a dose dependent and noncompetitive manner. The plots are representative of twenty-seven (■), nine (○), six (□), three (◊) and three (▲,▼,♦,●) determinations, respectively, where the error bars represent the standard deviation (S.D.) values.

Table 1
Inhibitory potency of 18-MC, ibogaine, and PCP on human muscle embryonic AChRs obtained by Ca^{2+} influx measurements.

NCA	Pre-incubation time (min)	IC_{50}[a] (μM)	n_H[b]
18-MC	5	6.8 ± 0.8	1.56 ± 0.15
	240	3.2 ± 1.7	1.90 ± 0.20
	1440	2.8 ± 1.1	1.61 ± 0.13
Ibogaine	5	17.0 ± 3.0	2.00 ± 0.29
PCP	5	31.0 ± 2.0	2.30 ± 0.04

[a] Required drug concentration to produce 50% inhibition of agonist-activated AChR ion channel flux, obtained from Fig. 1.
[b] Hill coefficient.

and ~4-fold more potent than PCP (Table 1). Our results also indicate that 18-MC inhibits the hα1β1γδ AChR in a dose dependent and noncompetitive manner (Fig. 1C). Interestingly, longer pre-incubation periods increase the potency of 18-MC by ~2-fold (Fig. 1B; Table 1). The same effect was observed either at 4 or 24 h pre-incubation. An obvious explanation is that the AChR is desensitized in the prolonged presence of 18-MC, and thus, the affinity and potency of 18-MC is increased. However, we cannot rule out other pleiotropic mechanisms such as modulation of AChR phosphorylation.

3.2. Equilibrium binding of [^{3}H]18-MC to the Torpedo AChR

In a first attempt to study the interaction of 18-MC with the muscle-type AChR ion channel, the affinity of [^{3}H]18-MC binding to *Torpedo* AChR membranes was determined. Fig. 2A shows the total (in the absence of 18-MC), nonspecific (in the presence of 100 μM 18-MC), and specific (total − nonspecific) [^{3}H]18-MC binding to *Torpedo* AChR membranes in the desensitized/CCh-bound state. Fig. 2B shows the Rosenthal–Scatchard plot for this specific binding. The results indicate that the *Torpedo* AChR ion channel has a single [^{3}H]18-MC binding site (stoichiometric ratio = 0.86 ± 0.13 binding sites/AChR) of relatively high affinity ($K_d = 0.23 \pm 0.04$ μM).

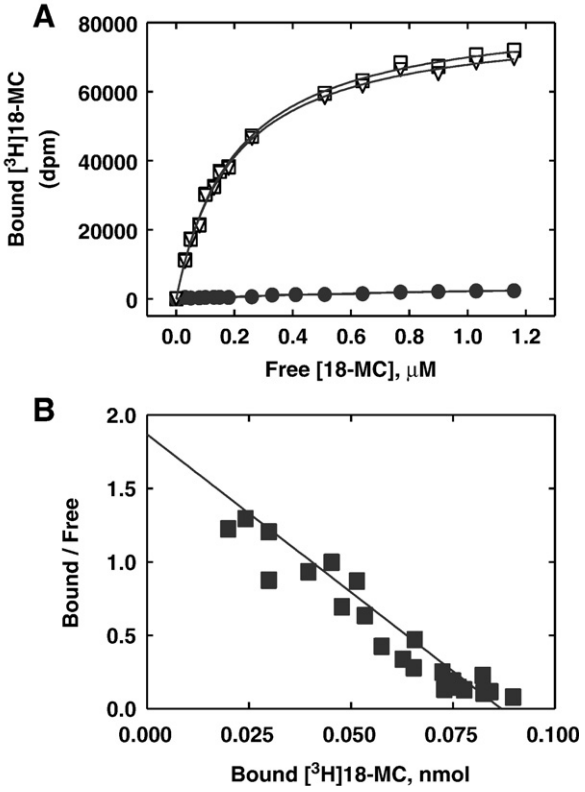

Fig. 2. Equilibrium binding of [^{3}H]18-MC to *Torpedo* AChRs in the desensitized/CCh-bound state. (A) Total (□), nonspecific (●) (in the presence of 100 μM 18-MC), and specific (○) (total − nonspecific binding) [^{3}H]18-MC binding. *Torpedo* AChR native membranes (0.5 μM) were suspended in BS buffer, in the presence of 1 mM CCh, and pre-incubated for 30 min at RT. Then, the total volume of the membrane suspensions (total and nonspecific binding) was divided into aliquots and increasing concentrations of [^{3}H]18-MC + 18-MC (i.e., 0.07 to 1.2 μM) were added to each tube and incubated for 2 h at RT. Finally, the AChR-bound [^{3}H]18-MC was separated from the free ligand by using the filtration assay described in Section 2.4. (B) Rosenthal–Scatchard plot for [^{3}H]18-MC specific binding to the *Torpedo* AChR ion channel. The K_d value (0.23 ± 0.04 μM) was determined from the negative reciprocal of the slope, according to Eq. (1). The stoichiometric ratio (0.86 ± 0.13 binding sites/AChR) was obtained from the *x*-intersect (when $y = 0$) of the plot $[B]/[F]$ *versus* $[B]$ according to Eq. (1), considering the AChR concentration in the assay. Shown is the combination of two separate experiments.

3.3. Radioligand competition binding results

Since the PCP/TCP binding sites have been previously characterized in muscle-type AChRs [14–19], we wanted to determine the location of the 18-MC binding site relative to this domain. To this end, we first determined the influence of 18-MC (Fig. 3A), ibogaine (Fig. 3A), and PCP (Fig. 3C) on [^{3}H]18-MC binding to *Torpedo* AChRs in the resting/α-bungarotoxin (α-BTx)-bound and desensitized/CCh-bound states. And, vice versa, the effect of 18-MC on [^{3}H]TCP (Fig. 4A) and [^{3}H]ibogaine (Fig. 4B) binding to the *Torpedo* AChR was also determined. 18-MC inhibits ~100% the specific binding of [^{3}H]TCP (Fig. 3A) and of [^{3}H]ibogaine (Fig. 3B), and PCP inhibits ~100% the specific binding of [^{3}H]18-MC (Fig. 3C) in both conformational states. Comparing the K_i values in different conformational states (Table 2), we can indicate that 18-MC binds to the [^{3}H]TCP binding site with ~8-fold higher affinity in the desensitized AChR than that in the resting AChR. These experiments are in agreement with the [^{3}H]18-MC competition results indicating that 18-MC binds to the desensitized AChR with ~2-fold higher affinity compared to that for the resting AChR (Table 2). The K_i value for 18-MC obtained by [^{3}H]ibogaine competition experiments is in the same concentration range as that obtained by [^{3}H]TCP and [^{3}H]18-MC competition experiments, respectively (Table 2). The results from the [^{3}H]18-MC competition experiments indicate that ibogaine binds to this locus with similar affinity for the resting and desensitized AChRs (Table 2).

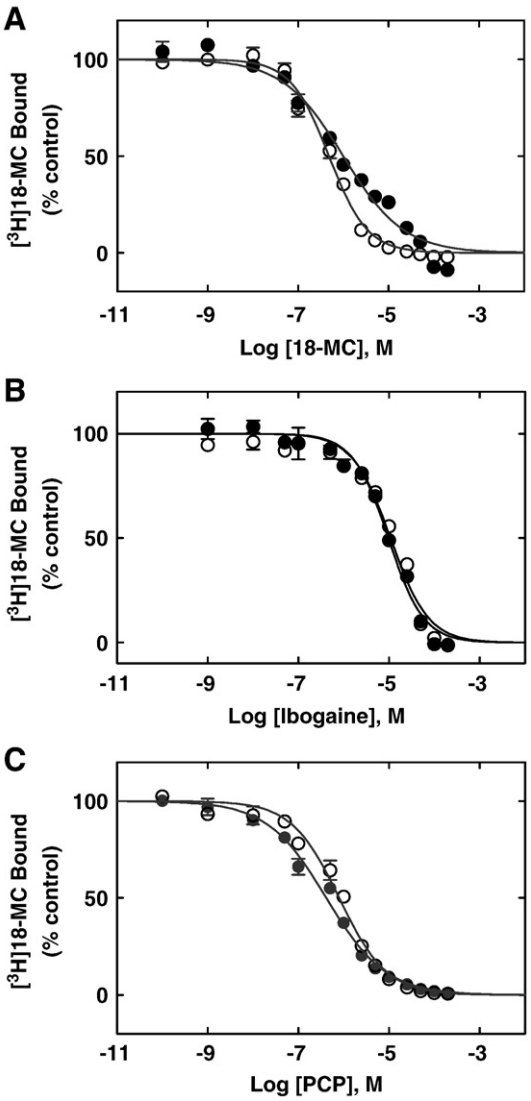

Fig. 3. (A) Inhibition of [^{3}H]18-MC binding to *Torpedo* AChRs in different conformational states by (A) 18-MC, (B) ibogaine, and (C) PCP, respectively. AChR-rich membranes (0.3 μM) were equilibrated (2 h) with 3.6 (●) or 5.5 nM (○) [^{3}H]18-MC, in the presence of 1 mM CCh (●) (desensitized/CCh-bound state) or 1 μM α-BTx (○) (resting/α-BTx-bound state), respectively, and increasing concentrations of the NCA under study. Nonspecific binding was determined in the presence of 50 (●) or 100 μM 18-MC (○), respectively. Each plot is the combination of two separated experiments each one performed in triplicate, where the error bars represent the standard deviation (S.D.) values. From these plots the IC_{50} and n_H values were obtained by nonlinear least-squares fit according to Eq. (2). Subsequently, the K_i values were calculated using Eq. (3). The calculated K_i and n_H values are summarized in Table 2.

The results from the complementary experiments indicate that PCP binds to the [^{3}H]18-MC site with practically the same affinity ($K_i = 0.41 \pm 0.03$ μM in the desensitized state, and 0.73 ± 0.05 μM in the resting state; see Table 2) as previously observed by [^{3}H]TCP equilibrium binding experiments in the desensitized (0.25 ± 0.05 μM; [28]) and resting (0.83 ± 0.05 μM; [15]) AChRs, respectively.

The fact that the calculated n_H values for 18-MC, ibogaine, and PCP are close to unity (Table 2) indicates that 18-MC inhibits [^{3}H]18-MC, [^{3}H]TCP and [^{3}H]ibogaine binding, and that PCP inhibits [^{3}H]18-MC binding, in a non-cooperative manner. These data suggest that ibogaine analogs and PCP interact with a single binding site, and that these drugs probably inhibit radioligand binding in a steric fashion.

3.4. Schild-type plots for 18-MC-induced inhibition of [^{3}H]TCP binding

Although the previous competition binding results suggest that 18-MC inhibits [^{3}H]TCP (Fig. 4A) binding to the desensitized *Torpedo* AChR in a steric fashion, we cannot rule out that this competition is produced by a potent allosteric mechanism as well. In this regard, we determined whether 18-MC inhibits [^{3}H]TCP binding to the desensitized AChR in a steric or allosteric manner by Schild-type analyses [30]. Fig. 5A shows the 18-MC-induced inhibition of [^{3}H]TCP binding at different initial concentrations of unlabeled PCP (i.e., 0, 3.1, 6.3, and 9.4 μM). At increased initial PCP concentrations, the plots were shifted to the right, indicating that higher 18-MC amounts are required to inhibit the binding of [^{3}H]TCP at increased PCP concentrations (see Fig. 5A). By means of a modified Schild-type plot (Fig. 5B) (see [14]), we found a linear relationship between the initial concentration of PCP and the extent of radioligand inhibition with a goodness of fit value (r^2) of 0.92 (Fig. 4B). Based on Schild-type analyses [30], a linear relationship ($r^2 > 0.6$) suggests that 18-MC inhibits [^{3}H]TCP binding to the desensitized/CCh-bound AChR by a steric mechanism. A r^2 value lower than 0.6 would indicate that there is no linear relationship and thus, that the inhibition is mediated by an allosteric mechanism. Based on the steric mechanism of inhibition elicited by 18-MC, we may infer that the 18-MC locus overlaps the PCP binding site within the *Torpedo* AChR ion channel in the desensitized state.

3.5. Ibogaine analog-induced enhancement of [^{3}H]cytisine binding to Torpedo AChRs

In order to determine the mechanisms of inhibition elicited by ibogaine analogs (e.g., receptor desensitization), we studied the effect of 18-MC and ibogaine on the binding of the agonist [^{3}H]cytisine to AChRs in the resting but activatable state. Fig. 6 shows that both ibogaine analogs enhance [^{3}H]cytisine binding to *Torpedo* AChRs in the resting but activatable state. A potential explanation for this pharmacological effect is based on the fact that cytisine binds with different affinity to the resting and desensitized AChRs [24], and that the AChR membrane suspension contains an excess of agonist binding sites (0.6 μM) compared with the initial concentration of [^{3}H]cytisine (7.7 nM). Since the cytisine K_i in the resting state is 1.6 μM [24], only a small fraction of AChRs will be initially labeled with [^{3}H]cytisine. Using Eq. (2), and considering $n_H = 1$, a fractional occupancy (θ) of ~0.005% for [^{3}H]cytisine bound to the resting AChR was calculated.

Table 2
Binding affinity of 18-MC, ibogaine, and PCP for the *Torpedo* AChR in different conformational states.

Radioligand	NCA	Desensitized/CCh-bound state			Resting/α-BTx-bound state		
		K_i[a] (μM)	n_H[b]	ΔG^c (kJ mol^{-1})	K_i[a] (μM)	n_H[b]	ΔG^c (kJ mol^{-1})
[^{3}H]TCP	18-MC	0.17 ± 0.01	1.11 ± 0.07	−38.6 ± 0.1	1.4 ± 0.1	0.89 ± 0.06	−33.4 ± 0.2
[^{3}H]Ibogaine	18-MC	0.61 ± 0.08	1.02 ± 0.13	−35.5 ± 0.3	ND	ND	ND
[^{3}H]18-MC	18-MC	0.47 ± 0.03	1.02 ± 0.06	−36.1 ± 0.2	1.0 ± 0.1	0.70 ± 0.05	−34.3 ± 0.3
	Ibogaine	9.3 ± 0.6	1.11 ± 0.07	−28.7 ± 0.2	11 ± 1	1.04 ± 0.08	−28.3 ± 0.2
	PCP	0.41 ± 0.03	0.76 ± 0.03	−36.4 ± 0.1	0.73 ± 0.05	0.88 ± 0.05	−35.0 ± 0.2

ND, not determined.
[a] Values were calculated from Fig. 3A–C ([^{3}H]18-MC competition experiments), Fig. 4A ([^{3}H]TCP competition experiments), and Fig. 4B ([^{3}H]ibogaine competition experiments), respectively, using Eq. (3).
[b] Hill coefficient.
[c] Values were calculated using Eq. (4), at the experimental temperature (298K).

Thus, if the AChR is shifted to its high affinity state (i.e., the desensitized state), an increase in the fraction of AChR-bound [^{3}H] cytisine molecules can be expected. In this regard, using Eq. (2), and considering that the cytisine K_i in the desensitized state is 0.45 μM [24], a fractional occupancy of ~0.017% for [^{3}H]cytisine bound to the desensitized AChR was obtained. This is an increase of ~3-fold in fractional occupancy. Coincident with this calculation, our binding results indicate an increase of ~2–2.5 times (see Fig. 6). The explanation of our results is that when the ibogaine analog binds to the ion channel, the AChR becomes desensitized thus, the affinity of [^{3}H]cytisine is increased and subsequently, a larger fraction of AChR-bound [^{3}H]cytisine is observed. In order to quantify this enhanced binding, the drug concentration to produce 50% increase of [^{3}H] cytisine binding was calculated. The apparent EC_{50}s values are 28 ± 10 and 0.3 ± 0.1 μM for ibogaine and 18-MC, respectively. These data indicate that ibogaine analogs enhance [^{3}H]cytisine binding probably by inducing AChR desensitization, and that 18-MC is ~90-fold more potent than ibogaine to induce AChR desensitization.

3.6. Binding kinetics of 18-MC determined by non-linear chromatography

Non-linear chromatography results permitted us to determine the k_{off} and K_a values according to Eqs. (5) and (6), respectively, and thus, to further calculate the k_{on} value for 18-MC when they bind to the *Torpedo* AChR in different conformational states (see Table 3). The results indicate that the dissociation rate constant (k_{off}) of 18-MC was slightly slower (0.077 ± 0.001 s^{-1}) when the column was exposed to (±)-epibatidine (the AChR is mainly in the desensitized state) compared to that exposed to α-BTx (the AChR is mainly in the resting state; see [26]) (0.109 ± 0.005 s^{-1}). This result indicates that 18-MC is dissociated from

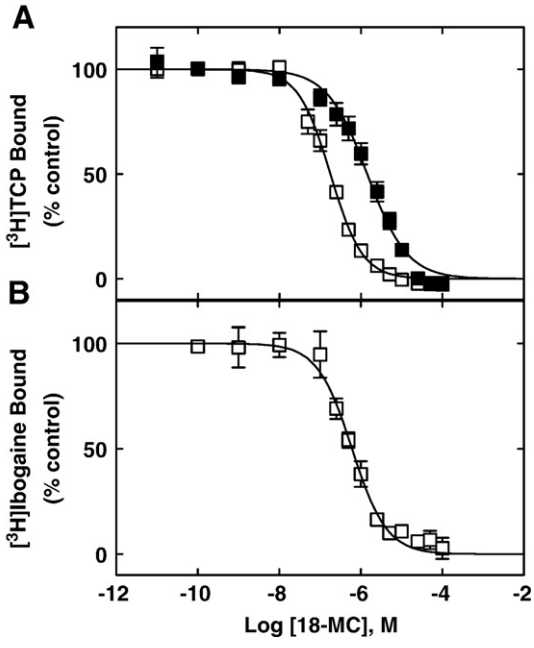

Fig. 4. 18-MC-induced inhibition of (A) [^{3}H]TCP and (B) [^{3}H]ibogaine binding to *Torpedo* AChRs in different conformational states. AChR-rich membranes (0.3 μM) were equilibrated (2 h) with 4 nM [^{3}H]TCP in the presence of 1 mM CCh (□) (desensitized/CCh-bound state) or 1 μM α-BTx (■) (resting/α-BTx-bound state), or alternatively with 19 nM [^{3}H]ibogaine in the presence of 1 mM CCh (□), and increasing concentrations of 18-MC. Nonspecific binding was determined in the presence of 100 μM PCP. Each plot is the combination of two separated experiments each one performed in triplicate, where the error bars represent the standard deviation (S.D.) values. From these plots the IC_{50} and n_H values were obtained by nonlinear least-squares fit according to Eq. (2). Subsequently, the K_i values were calculated using Eq. (3). The calculated K_i and n_H values are summarized in Table 2.

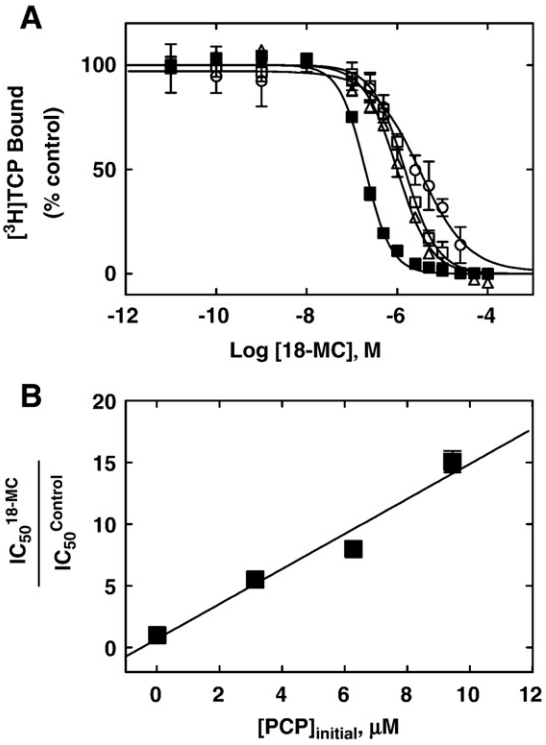

Fig. 5. Schild-plot for 18-MC-induced inhibition of [^{3}H]TCP binding to the *Torpedo* AChR in the desensitized/CCh-bound state. (A) AChR-rich membranes (0.3 μM nAChR) were equilibrated with [^{3}H]TCP, in the presence of 1 mM CCh (desensitized state), at initial PCP concentrations of 0 (control; ■), 3.1 (△), 6.3 (□), and 9.4 μM (○), respectively. The apparent IC_{50} values were calculated by nonlinear least-squares fit according to Eq. (2). Shown is the average of experiments performed in triplicate. (B) Modified Schild-plot for 18-MC-induced inhibition of [^{3}H]TCP binding. The plot shows a linear relationship with a r^2 value of 0.92. Shown is the result of experiments performed in triplicate, where the error bars represent the standard deviation (S.D.) values.

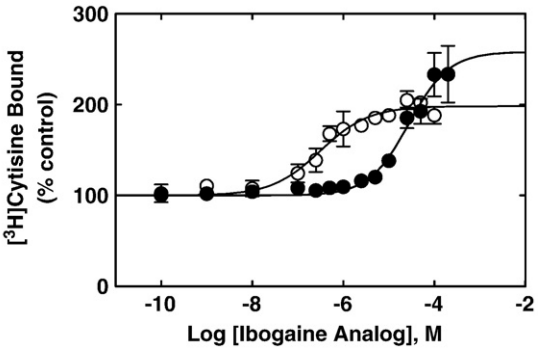

Fig. 6. Ibogaine analog-induced enhancement of [^{3}H]cytisine binding to *Torpedo* AChRs in the resting but activatable state. AChR native membranes (0.3 μM nAChR) were equilibrated (30 min) with 7.7 nM [^{3}H]cytisine, and increasing concentrations of ibogaine (●) and 18-MC (○), respectively. Each plot is the combination of 2–3 separated experiments each one performed in triplicate, where the error bars represent the standard deviation (S.D.) values. The apparent EC_{50} values, obtained according to Eq. (2), were 28 ± 10 (apparent $n_H = 0.99 \pm 0.22$) and 0.3 ± 0.1 μM (apparent $n_H = 0.81 \pm 0.20$) for ibogaine and 18-MC, respectively.

the desensitized *Torpedo* AChR ion channel at a slower rate than that from the resting AChR ion channel. This explains the pharmacological mechanism by which 18-MC binds to its own site with ~2-fold higher affinity to the desensitized AChR compared to the resting AChR (see Table 2).

3.7. Thermodynamic parameters for the interaction of 18-MC with the Torpedo AChR

In previous studies, an increase in the temperature changed the chromatographic retention of several NCAs including dextromethorphan and levomethorphan [36], and bupropion [22]. Thus, the temperature-dependent results can then be analyzed using the van't Hoff plot (see Eq. (7)) to calculate the changes in enthalpy ($\Delta H°$) and entropy ($\Delta S°$) associated with the interactions of 18-MC with the immobilized AChR. In this study, increasing temperatures produced significant changes in the retention of 18-MC on the CMAC-*Torpedo* AChR column in the presence of either α-BTx (resting state; see [26]) or (±)-epibatidine (desensitized state), respectively. Since the resulting van't Hoff plots were linear (Fig. S1A in the Supplementary data), the thermodynamic parameters $\Delta H°$ and $\Delta S°$ were calculated from the slopes and intercepts of the van't Hoff plots, respectively, according to Eq. (7), whereas ΔG^{20} was calculated according to Eq. (8) (Table 4). The linearity of the van't Hoff plots indicates an invariant retention mechanism over the temperature range studied [36,37].

The thermodynamic results indicate that the $\Delta H°$ and $-T\Delta S°$ values obtained for 18-MC in the resting AChR are practically in the same energetic range, whereas the enthalpic contribution is more than 2-fold higher than the entropic contribution in the desensitized AChR (Table 4). This indicates that the enthalpic contribution is more important in the desensitized state compared to that in the resting state. Since negative $\Delta H°$ values suggest the existence of attractive forces (e.g., van der Waals, hydrogen bond, and electrostatic interactions) (reviewed in [1]), the interactions between 18-MC and the ion channel are stronger when the AChR becomes desensitized, increasing the stability of the molecule within the ion channel in this particular state. This is in agreement with higher ΔG values for the desensitized AChR compared with that for the resting AChR obtained by radioligand binding assays (Table 2). On the other hand, the local conformational changes or solvent reorganization in the binding pocket of the resting AChR elicited by 18-MC is more pronounced than that in the desensitized AChR binding site.

Since only small changes in the kinetic parameters for 18-MC between the resting/α-BTx-bound and desensitized/epibatidine-bound states at 20 °C were observed (see Table 3), additional studies were conducted in the 10–25 °C temperature range. In this regard, Arrhenius plots were constructed using the determined k_{off} values (see Eq. (5)) for 18-MC at different temperatures (Fig. S1B in the Supplementary data). Since the Arrhenius plots are different from zero, the drug dissociation process is mediated mainly by an enthalpic component. To quantify this component, the E_a value was first calculated from the Arrhenius plots (see Eq. (9)), and the ΔH^+ value was subsequently calculated using Eq. (10) (Table 4). The fact that the E_a value in the desensitized state is higher than that in the resting state indicates that the energy barrier for drug dissociation from the desensitized ion channel is higher than that from the resting ion channel. This correlates well with a higher ΔH^+ value in the desensitized state compared to that in the resting state.

Table 3
Kinetic and thermodynamic parameters of 18-MC binding to *Torpedo* AChRs in different conformational states determined by non-linear chromatography studies.

Parameter	α-BTx treated column[a]	Epibatidine treated column[b]
k_{off} (s^{-1})[c]	0.109 ± 0.005	0.077 ± 0.001
k_{on} (s^{-1} μM^{-1})	0.123 ± 0.002	0.228 ± 0.003
K_a (μM^{-1})[d]	1.13 ± 0.04	2.97 ± 0.01
ΔG^{20} (kJ mol^{-1})[e]	−33.9 ± 0.1	−36.3 ± 0.1

The CMAC-*Torpedo* AChR column was pre-treated with either α-BTx[a] (the AChR is mainly in the resting state) or (±)-epibatidine[b] (the AChR is mainly in the desensitized state).
[c,d]Constants were empirically determined using Eqs. (5) and (6), respectively, whereas the k_{on} values were calculated as $k_{on} = k_{off} \cdot K_a$.
[e]Values were calculated using Eq. (4).

Table 4
Thermodynamic parameters of 18-MC binding to *Torpedo* AChRs in different conformational states determined by non-linear chromatography.

Thermodynamic parameters	α-BTx treated column[a]	Epibatidine treated column[b]
$\Delta H°$ (kJ mol^{-1})[c]	−18.5 ± 1.1	−25.0 ± 1.1
$-T\Delta S°$ (kJ mol^{-1})[d]	−15.5 ± 1.1	−11.2 ± 1.2
ΔG^{20} (kJ mol^{-1})[e]	−34.0 ± 1.4	−36.3 ± 1.4
E_a (kJ mol^{-1})[f]	16.4 ± 0.7	22.4 ± 1.5
ΔH^+ (kJ mol^{-1})[g]	13.9 ± 0.7	20.0 ± 1.5

The CMAC-*Torpedo* AChR column elution was performed in the presence of either α-BTx[a] (the AChR is mainly in the resting state) or (±)-epibatidine[b] (the AChR is mainly in the desensitized state).
[c,d]The thermodynamic parameters $\Delta H°$ and $\Delta S°$ were calculated from Fig. 1A (see Supplementary data) according to Eq. (7).
[e]Values were calculated using Eq. (8).
[f]Values for the process of drug dissociation were obtained from Fig. 1B (see Supplementary data) according to Eq. (9).
[g]Values were calculated using Eq. (10).

3.8. Molecular docking of 18-MC in Torpedo and human muscle AChR ion channels

18-MC in the neutral and protonated states was docked to models of human muscle (Fig. 7A) and *Torpedo* (Fig. 7B) ion channels, respectively. Molegro Virtual Docker generated a series of docking poses and ranked them using energy-based criterion using the embedded scoring function MolDockScore. Based on this ranking, the lowest energy pose of the AChR–ligand complexes was selected and shown in Fig. 7. In both models, the docked 18-MC molecule interacted exclusively with the M2 helices provided by each subunit, and no interactions with other transmembrane helices were observed. More specifically, 18-MC interacted with the luminal domain formed between the serine (position 6′) and valine (position 13′) rings. However, M2 helices are quite dissimilar when amino acid sequences of respective AChR subunits from *Torpedo* and humans are considered, especially in residues from the rings exposed to the center of the channel. For instance, in the serine ring (position 6′), both β1-

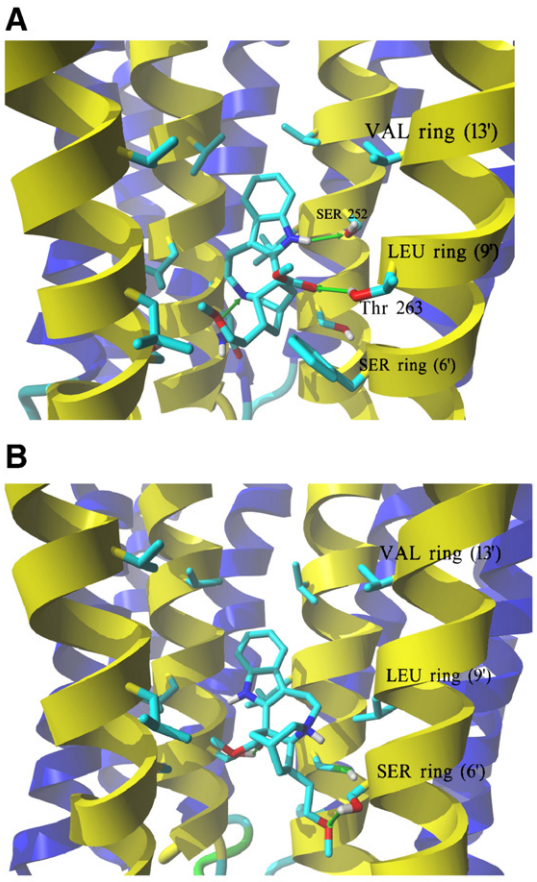

Fig. 7. Complexes formed between 18-MC and AChR ion channel models obtained by molecular docking. (A) Side view of the lowest energy complex formed between neutral 18-MC and the human muscle AChR ion channel. Receptor subunits are shown in the secondary structure mode (M2 helices, yellow; other transmembrane helices, blue) with residues forming the serine (SER) (position 6′), leucine (LEU) (positions 9′), and valine (VAL) (position 13′) rings, shown explicitly in stick mode. Green arrows indicate hydrogen bonds formed between the pyrrole amino group and the α1-Ser252 residue (position 10′), another between the ligand ionizable amino group and γ-Asn257 at the SER ring, and a third one between the carbonyl of the ester group and β1-Thr263 (position 10′). A similar interaction was obtained for protonated 18-MC. (B) Side view of the lowest energy complex formed between protonated 18-MC and the *Torpedo* AChR ion channel. The subunit γ was hidden for clarity, and the order of the remaining subunits is (from the left): α1, β1, δ, α1. The ether and ester groups from 18-MC form hydrogen bonds with two Ser residues, each one from the respective α1 and β1 subunits, forming the SER ring. Another strong hydrogen bond interaction is observed between the charged amino group and the same α1-Ser residue. 18-MC interacts with the LEU and VAL rings by additional weaker van der Waals contacts. A similar interaction was obtained for neutral 18-MC.

Ser245 and γ-Ser249 residues from *Torpedo* AChR are exchanged into the respective Phe and Asn residues in the human muscle subtype, whereas the *Torpedo* δ-Cys247 is exchanged into Ser in the human model. Docking results indicate that the binding orientation of the 18-MC molecule in the complex differs depending on the model used (*Torpedo versus* human).

In the case of the interaction between neutral 18-MC and the human muscle AChR ion channel model (Fig. 7A), three hydrogen bonds interacting with 18-MC can be found: one between the pyrrole amino group and the α1-Ser252 residue (position 10′), another between the ligand ionizable amino group and γ-Asn257 (position 6′), and a third one between the carbonyl of the ester group and β1-Thr263 (position 10′). The latter two residues are not present at these positions in the *Torpedo* AChR ion channel model, and this difference seems to be responsible for the observed complex divergences. A similar orientation for the protonated version of 18-MC was observed in docking to the human muscle AChR model.

A different position with optimized interactions is found for neutral 18-MC docked in the *Torpedo* AChR ion channel (Fig. 7B) compared to that for the human muscle AChR ion channel (Fig. 7A). The calculated docking energy (MolDockScore values) for the human muscle AChR (−119.6 and −116.1 kJ/mol for the neutral and protonated form, respectively) is very similar as that for the *Torpedo* AChR (−113.8 and −110.4 kJ/mol for the neutral and protonated form, respectively). Although 18-MC interacts with each AChR channel with practically the same binding energy, its luminal orientation is different in both complexes. In the *Torpedo* AChR ion channel, the ligand is oriented in a manner allowing its ether and ester groups to form hydrogen bonds with two Ser residues, each one from the respective α1 and β1 subunits, forming the serine ring (position 6′) (Fig. 7B). Another strong hydrogen bond interaction can be observed between the charged amino group and the same α1-Ser residue. In addition, 18-MC interacts with non-polar residues by weak van der Waals contacts ranging from the leucine (position 9′) to valine (position 13′) rings. Essentially the same mode of interaction was observed for the protonated version of the molecule.

4. Discussion

Ibogaine analogs pharmacologically behave as NCAs of several AChRs [6–10]. However, we do not have a complete understanding of how these drugs interact with the AChR ion channel in different conformational states. In this regard, this study is an attempt to characterize the interactions of 18-MC with the archetype of the Cys-loop ligand-gated ion channels superfamily, the muscle-type AChR, in distinct conformational states, and to compare them with that for PCP, a well known NCA. To this end, radioligand binding assays, Ca^{2+} influx, kinetic and thermodynamic measurements, and molecular modeling and docking studies were performed. Although this study does not directly address the anti-addictive properties of ibogaine analogs, the results of this work should ultimately provide a better understanding of how these compounds interact with the AChR, and will bestow the basic knowledge to afford the study of the interaction of these compounds with neuronal-type AChRs, more suitable targets for the anti-addictive action of these compounds.

4.1. 18-MC interaction with the agonist-activated AChR ion channel

The effect of 18-MC on (±)-epibatidine-activated Ca^{2+} influx in TE671 cells was compared to that for ibogaine and PCP using a pre-incubation protocol (Fig. 1A). Ibogaine and PCP showed inhibitory potencies similar to that determined previously by $^{86}Rb^{+}$ efflux experiments using the same cell type [7], but they were ~2- and ~4-fold less potent than 18-MC (see Table 1). Interestingly, the opposite ratio was observed in the α3β4 AChR, where 18-MC and ibogaine inhibit this receptor type with IC_{50} values of 0.75–0.90 and 0.22 μM, respectively [8,9]. This is the first time where the interaction of 18-MC with muscle AChRs is demonstrated, supporting the view that ibogaine analogs inhibit AChRs in a noncompetitive manner (see Fig. 1C). Based on our own results and on the inhibitory potency of 18-MC for other AChR types [8,9], the following AChR specificity sequence was obtained: α3β4 (0.75–0.90 μM)>α1β1γδ (6.8 μM)>α4β2 (>20 μM).

The fact that the n_H values for 18-MC, ibogaine, and PCP are higher than unity (see Table 1) indicates that the inhibitory process is produced in a cooperative manner, suggesting that there are potentially more than one binding site for these NCAs in the activated muscle AChR ion channel or that there are more than one mechanism of inhibition. In this regard, our [^{3}H]cytisine results indicate that ibogaine analogs induce an enhancement of agonist binding to the resting but activatable AChR (Fig. 6), suggesting that the analogs may

induce AChR desensitization. This is supported by the observed higher potency of 18-MC when it is pre-incubated for long periods (4 and 24 h) (Table 1). Finally, there is a good correlation between the IC_{50} (Table 1) and apparent EC_{50} values, indicating that 18-MC is more potent than ibogaine inhibiting Ca^{2+} influx as well as enhancing [^{3}H] cytisine binding, respectively.

4.2. 18-MC interaction with the desensitized and resting AChR ion channels

The results from the [^{3}H]TCP competition binding experiments indicate that 18-MC binds with ~8-fold higher affinity to the desensitized/CCh-bound *Torpedo* AChR compared to the resting/α-BTx-bound AChR (see Table 2). The calculated K_i value for 18-MC (0.17 ± 0.01 μM; see Table 2) obtained in the [^{3}H]TCP competition binding experiments when the AChR is in the desensitized/CCh-bound state is practically the same as that determined by equilibrium binding ($K_d = 0.23 \pm 0.04$ μM; see Fig. 2). The observed higher affinity of 18-MC for the [^{3}H]TCP locus in the desensitized AChR is corroborated by the [^{3}H]18-MC competition results (Table 2). The observed higher affinity of 18-MC for the desensitized AChR corresponds very well with its high desensitizing potency. In this regard, a potential mechanism can be envisioned where 18-MC first induces AChR desensitization and in this conformational state, the drug is maintained for longer time in the bound state (i.e., see smaller k_{off} value in Table 3). Since this hypothetic scheme adds a new dimension to the inhibitory mechanisms elicited by ibogaine analogs, further experiments deserve to be performed to support this possibility.

The radioligand competition experiments also indicate that 18-MC inhibits the binding of [^{3}H]TCP (the structural and functional analog of PCP) and vice versa, that PCP inhibits the binding of [^{3}H]18-MC to desensitized/CCh-bound AChRs with n_H values close to unity (Table 2). This suggests that both drugs may be interacting with a single binding site in the desensitized AChR. Although this evidence suggests a steric mode of competition between 18-MC and PCP, we cannot rule out the possibility of a strong allosteric effect as well. In this regard, Schild-type analyses indicate that 18-MC displaces [^{3}H]TCP binding from its site in the desensitized/CCh-bound state AChR by a steric mechanism (Fig. 5). These data suggest that the 18-MC binding site overlaps the high affinity PCP locus in the desensitized AChR. This conclusion is supported by our molecular docking results. The analysis of the obtained molecular complexes clearly indicates that 18-MC in either the neutral or protonated form (see Fig. 7) binds to the middle portion of both muscle AChR ion channels (human and *Torpedo*) between the serine (position 6′) and valine (position 13′) rings. Molecular docking results also demonstrate the existence of a network of hydrogen bond interactions between different 18-MC moieties and several residues located at the serine ring (position 6′) and at position 10′, as well as additional van der Waals interactions with the adjacent serine (position 6′), leucine (position 9′), and valine (position 13′) rings (see Fig. 7B). In turn, these results are in agreement with the postulated location of the PCP binding site in the desensitized AChR ion channel. For instance, photoaffinity labeling [18,38] and molecular docking [17] studies indicated that the PCP locus is located between the threonine (position 2′) and leucine (position 9′) rings. The same basic results were obtained for several antidepressants in muscle AChR ion channels [17,22,24]. In conclusion, our data agree with a model where overlapping binding sites exist for ibogaine analogs, PCP, and antidepressants, in the desensitized AChR ion channel.

The radioligand binding results using AChRs in the resting state indicate that 18-MC interacts with the [^{3}H]18-MC locus with practically the same affinity (1.0 ± 0.1 μM) as that for the [^{3}H]TCP site (1.4 ± 0.1 μM) (see Table 2). Considering that these competition results present n_H values close to unity, we suggest that there exist overlapping binding sites for ibogaine analogs and PCP. Interestingly, the thermodynamic studies support the notion that the interaction of 18-MC with the resting AChR ion channel (i.e., mixed enthalpic–entropic) is different to that with the desensitized AChR ion channel (i.e., more enthalpic than entropic). This difference suggests that attractive forces are more important than local conformational changes or solvent reorganization in the 18-MC binding pocket of the desensitized AChR compared to the resting AChR. Previous thermodynamic studies indicated that bupropion [22] and PCP [39] interact with the *Torpedo* AChR ion channel by entropy-driven mechanisms. The contrasting result obtained in the desensitized state suggests that 18-MC interacts with its binding site by mechanisms different to that for bupropion and PCP.

Considering the above results, we envision a mechanistic process where 18-MC first binds to its site in the resting AChR ion channel with relatively low affinity. Subsequently, 18-MC blocks the activated (open) channel and induces receptor desensitization increasing its affinity for the desensitized ion channel. In this conformational state, 18-MC interacts with a binding domain located between the serine and valine rings that is shared by antidepressants and PCP. The formation of hydrogen bonds with the serine ring and additional van der Waals contacts with the serine, leucine, and valine rings, finally decreases the dissociation of 18-MC from the desensitized ion channel. Our results also suggest that ibogaine analogs can inhibit muscle AChRs by a combination of several noncompetitive inhibitory mechanisms including, ion channel blocking and AChR desensitization.

Acknowledgements

This research was supported by grants from the Science Foundation Arizona and Stardust Foundation and from the Office of Research and Sponsored Programs, Midwestern University (to H.R.A.), by a grant from the Polish Ministry of Science and Higher Education (no. NN 405297036) and by the FOCUS and TEAM research subsidy from the Foundation for Polish Science (to K.J.), and by the National Institute on Drug Addiction (NIDA) grant DA016283 (to S.D.G.). This research was also supported in part by the Intramural Research Program of the NIH, National Institute on Aging. The authors give thanks to NIDA (NIH, Bethesda, Maryland, USA) for the gift of [^{3}H] Ibogaine, ibogaine, and phencyclidine, and to Jorgelina L. Arias Castillo and Paulina Iacoban for their technical assistance.

Appendix A. Supplementary data

Supplementary data associated with this article can be found, in the online version, at doi:10.1016/j.bbamem.2010.03.013.

References

[1] H.R. Arias, Thermodynamics of nicotinic receptor interactions, in: R.B. Raffa (Ed.), Drug-Receptor Thermodynamics: Introduction and Applications, John Wiley & Sons, Ltd., USA, 2001, pp. 293–358.
[2] H.R. Arias, Ligand-gated ion channel receptor superfamilies, in: H.R. Arias (Ed.), Biological and Biophysical Aspects of Ligand-Gated Ion Channel Receptor Superfamilies, Research Signpost, Kerala, India, 2006, pp. 1–25.
[3] H.R. Arias, P. Bhumireddy, C. Bouzat, Molecular mechanisms and binding site locations for noncompetitive antagonists of nicotinic acetylcholine receptors, Int. J. Biochem. Cell Biol. 38 (2006) 1254–1276.
[4] E.X. Albuquerque, E.F.R. Pereira, A. Alkondon, S.W. Rogers, Mammalian nicotinic acetylcholine receptors: From structure to function, Physiol. Rev. 89 (2009) 73–120.
[5] S.M. Sine, A.G. Engel, Recent advances in Cys-loop receptor structure and function, Nature 440 (2006) 448–455.
[6] B. Badio, W.L. Padgett, J.W. Daly, Ibogaine: a potent noncompetitive blocker of ganglionic/neuronal nicotinic receptors, Mol. Pharmacol. 51 (1997) 1–5.
[7] J.D. Fryer, R.J. Lukas, Noncompetitive functional inhibition at diverse, human nicotinic acetylcholine receptor subtypes by bupropion, phencyclidine, and ibogaine, J. Pharmacol. Exp. Ther. 288 (1999) 88–92.

[8] S.D. Glick, I.M. Maisonneuve, B.A. Kitchen, M.W. Fleck, Antagonism of α3β4 nicotinic receptors as a strategy to reduce opioid and stimulant self-administration, Eur. J. Pharmacol. 438 (2002) 99–105.
[9] C.J. Pace, S.D. Glick, I.M. Maisonneuve, L.W. He, P.A. Jokiel, M.E. Kuehne, M.W. Fleck, Novel iboga alkaloid congeners block nicotinic receptors and reduce drug self-administration, Eur. J. Pharmacol. 492 (2004) 159–167.
[10] I.M. Maisonneuve, S.D. Glick, Anti-addictive actions of an iboga alkaloid congener: a novel mechanism for a novel treatment, Pharmacol. Biochem. Behav. 75 (2003) 607–618.
[11] S.D. Glick, R.L. Ramirez, J.M. Livi, I.M. Maisonneuve, 18-Methoxycoronaridine acts in the medial habenula and/or interpeduncular nucleus to decrease morphine self-administration in rats, Eur. J. Pharmacol. 537 (2006) 94–98.
[12] M.E. Kuehne, L. He, P.A. Jokiel, C.J. Pace, M.W. Fleck, I.M. Maisonneuve, S.D. Glick, J. M. Bidlack, Synthesis and biological evaluation of 18-methoxycoronaridine congeners. Potential antiaddiction agents, J. Med. Chem. 46 (2003) 2716–2730.
[13] H.R. Arias, Is the inhibition of nicotinic acetylcholine receptors by bupropion involved in its clinical actions? Int. J. Biochem. Cell Biol. 41 (2009) 2098–2108.
[14] H.R. Arias, E.A. McCardy, E.Z. Bayer, M.J. Gallagher, M.P. Blanton, Allosterically linked noncompetitive antagonist binding sites in the resting nicotinic acetylcholine receptor ion channel, Arch. Biochem. Biophys. 403 (2002) 121–131.
[15] H.R. Arias, J.R. Trudell, E.Z. Bayer, B. Hester, E.A. McCardy, M.P. Blanton, Noncompetitive antagonist binding sites in the *Torpedo* nicotinic acetylcholine receptor ion channel. Structure–activity relationship studies using adamantane derivatives, Biochemistry 42 (2003) 7358–7370.
[16] H.R. Arias, P. Bhumireddy, G. Spitzmaul, J.R. Trudell, C. Bouzat, Molecular mechanisms and binding site location for the noncompetitive antagonist crystal violet on nicotinic acetylcholine receptors, Biochemistry 45 (2006) 2014–2026.
[17] M. Sanghvi, A.K. Hamouda, K. Jozwiak, M.P. Blanton, J.R. Trudell, H.R. Arias, Identifying the binding site(s) for antidepressants on the *Torpedo* nicotinic acetylcholine receptor: [^{3}H]2-Azidoimipramine photolabeling and molecular dynamics studies, Biochem. Biophys. Acta 1778 (2008) 2690–2699.
[18] A.K. Hamouda, D.C. Chiara, M.P. Blanton, J.B. Cohen, Probing the structure of the affinity-purified and lipid-reconstituted *Torpedo* nicotinic acetylcholine receptor, Biochemistry 47 (2008) 12787–12794.
[19] M.J. Eaton, C. Labarca, V.A. Eterović, M2 Mutations of the nicotinic acetylcholine receptor increase the potency of the non-competitive inhibitor phencyclidine, J. Neurosci. Res. 61 (2000) 44–51.
[20] S.E. Pedersen, E.B. Dreyer, J.B. Cohen, Location of ligand-binding sites on the nicotinic acetylcholine receptor α-subunit, J. Biol. Chem. 261 (1986) 13735–13743.
[21] R. Moaddel, K. Jozwiak, K. Whittington, I.W. Wainer, Conformational mobility of immobilized α3β2, α3β4, α4β2, α4β4 nicotinic acetylcholine receptors, Anal. Chem. 77 (2005) 895–901.
[22] H.R. Arias, F. Gumilar, A. Rosenberg, K.M. Targowska-Duda, D. Feuerbach, K. Jozwiak, R. Moaddel, I.W. Weiner, C. Bouzat, Interaction of bupropion with muscle-type nicotinic acetylcholine receptors in different conformational states, Biochemistry 48 (2009) 4506–4518.
[23] S. Michelmore, K. Croskery, J. Nozulak, D. Hoyer, R. Longato, A. Weber, R. Bouhelal, D. Feuerbach, Study of the calcium dynamics of the human α4β2, α3β4 and α1β1γδ nicotinic acetylcholine receptors, Naunyn-Schmiedebergs Arch. Pharmacol. 366 (2002) 235–245.
[24] H.R. Arias, D. Feuerbach, P. Bhumireddy, M.O. Ortells, Inhibitory mechanisms and binding site locations for serotonin selective reuptake inhibitors on nicotinic acetylcholine receptors, Int. J. Biochem. Cell Biol. 42 (2010) 712–724.
[25] G. Scatchard, The attraction of proteins for small molecules and ions, Ann. N.Y. Acad. Sci. 51 (1949) 660–672.
[26] M.A. Moore, M.P. McCarthy, Snake venom toxins, unlike smaller antagonists, appear to stabilize a resting state conformation of the nicotinic acetylcholine receptor, Biochim. Biophys. Acta 1235 (1995) 336–342.
[27] Y. Cheng, W.H. Prusoff, Relationship between the inhibition constant (K_i) and the concentration of inhibitor which causes 50 percent inhibition (IC_{50}) of an enzymatic reaction, Biochem. Pharmacol. 22 (1973) 3099–3108.
[28] O.R. Pagán, V.A. Eterović, M. García, D. Vergne, C.M. Basilio, A.D. Rodríguez, R.M. Hann, Cembranoid and long-chain alkanol sites on the nicotinic acetylcholine receptor and their allosteric interaction, Biochemistry 40 (2001) 11121–11130.
[29] J. Malone, K. Jozwiak, H.R. Arias, Interaction of ibogaine analogs with the *Torpedo* nicotinic receptor, 48th Annual Meeting of the American Society for Cell Biology (ASCB), San Francisco, CA, USA, December 13–17 2008.
[30] H.O. Schild, p*Ax* and competitive drug antagonism, Br. J. Pharmacol. 4 (1949) 277–280.
[31] J.L. Wade, A.F. Bergold, P.W. Carr, Theoretical description of nonlinear chromatography, with applications to physicochemical measurements in affinity chromatography and implications for preparative-scale separations, Anal. Chem. 59 (1987) 1286–1295.
[32] K. Jozwiak, S. Ravichandran, J.S. Collins, I.W. Wainer, Interaction of noncompetitive inhibitors with an immobilized α3β4 nicotinic acetylcholine receptor investigated by affinity chromatography, quantitative–structure activity relationship analysis, and molecular docking, J. Med. Chem. 47 (2004) 4008–4021.
[33] R. Moaddel, K. Jozwiak, I.W. Wainer, Allosteric modifiers of neuronal nicotinic receptors: New methods, new opportunities, Med. Res. Rev. 27 (2007) 723–753.
[34] A. Miyazawa, Y. Fujiyoshi, N. Unwin, Structure and gating mechanism of the acetylcholine receptor pore, Nature 423 (2003) 949–955.
[35] N. Unwin, Refined structure of the nicotinic acetylcholine receptor at 4 Å resolution, J. Mol. Biol. 346 (2005) 967–989.
[36] K. Jozwiak, S. Hernandez, K.J. Kellar, I.W. Wainer, The enantioselective interactions of dextromethorphan and levomethorphan with the α3β4-nicotinic acetylcholine receptor: comparison of chromatographic and functional data, J. Chromatogr. B 797 (2003) 373–379.
[37] K. Jozwiak, J. Haginaka, R. Moaddel, I.W. Wainer, Displacement and nonlinear chromatographic techniques in the investigation of interaction of noncompetitive inhibitors with an immobilized α3β4 nicotinic acetylcholine receptor liquid chromatographic stationary phase, Anal. Chem. 74 (2002) 4618–4624.
[38] M.B. Pratt, S.E. Pedersen, J.B. Cohen, Identification of the sites of incorporation of [^{3}H]ethidium diazide within the *Torpedo* nicotinic acetylcholine receptor ion channel, Biochemistry 39 (2000) 11452–11462.
[39] R.E. Oswald, M.J. Bamberger, J.T. McLaughlin, Mechanism of phencyclidine binding to the acetylcholine receptor from *Torpedo* electroplaque, Mol. Pharmacol. 25 (1984) 360–368.